Tea Waste Products: A New Low-Cost and Green Adsorbent Alternative for Rhodamine-B Dye Removal

Meyliana Wulandari[1*], Nofrizal Syamsudin[2], and Syed Azhar Syed Sulaiman[3]

[1]*Department of Chemistry, Faculty of Science and Technology, State Islamic University (UIN) Syarif Hidyatullah Jakarta, Jl. Ir H. Juanda No. 95, Ciputat, Tangerang Selatan, Banten 15412, Indonesia*

[2]*Research and Development Center for Oil and Gas Technology – LEMIGAS, Jl. Ciledug Raya Kavling. 109, Jakarta 12230, Indonesia*

[3]*Department of Pharmaceutical Sciences, Universiti Sains Malaysia Minden, 11800 Penang, Malaysia*

* ***Corresponding author:***

tel: +62-81386050077
email: meylianawulandari@uinjkt.ac.id

Received: June 26, 2022
Accepted: October 21, 2022

DOI: 10.22146/ijc.75739

Abstract: *Tea waste products were thrown out without any intention to utilize their potential benefits. This waste will help to improve industries to absorb rhodamine-B (RhB) dye pollutants currently used by various industries. This study evaluated the application of tea waste products to remove Rh-B from aqueous systems by investigating adsorption kinetics in a batch process. The ability and mechanism of Indonesian black and green tea in RhB adsorption were determined by optimizing temperature, pH, contact time, and concentration of dye solution. Achievement of equilibrium attained at 40 min for black tea (BT) and green tea (GT). Subsequently, the adsorption capacity reached optimum at 80 and 70 °C for GT, and the maximum adsorption capacities for BT and GT were 22 and 47 mg/g, respectively, at pH 2.5. The absorption of RhB in both bio-sorbents was an exothermic process that well fit the Langmuir model and a pseudo-second-order reaction. The presented R^2 values from the Langmuir isotherm are 0.9967 (BT) and 0.9979 (GT). The separation factor was determined as 0.026 (BT) and 0.055 (GT). Thermodynamic studies were carried out to calculate free energy, enthalpy, and entropy changes. The result showed that the removal study of BT and GT is 59.06 and 60.25%, respectively, using 10% acetic acid. Study comparisons were carried out on both teas with other bio-sorbents for more improvement. These results show that tea waste products can be used as alternative adsorbents to absorb RhB from wastewater.*

Keywords: *biosorption; black tea; dye adsorption; green tea; rhodamine-B*

■ INTRODUCTION

Dyes define as complex organic compounds in many industries, such as textiles, plastics, rubbers, leathers, cosmetics, and papers [1]. Malachite green, methyl violet, azure dye, indigo carmine, and RhB are various textile dyes [2]. RhB, a synthetic dye, is commonly used in the textile industry. Come with the xanthine family, RhB can be applied extensively in biological, analytical, and optical sciences [3]. RhB, likewise other dyes, is steady even in contact with light, heat, and oxidation, and it is highly carcinogenic to animals and humans [4]. When RhB is straightly disclosed to the body, it can cause biological problems, i.e., inflammation, hemolysis, and decreased function liver and kidney. Getting rid of dye waste into the environment starts environmental destruction. Data shows that 100 tons of dyes release into the atmosphere annually and poison rivers, which will be challenging to be treated [1].

RhB is non-biodegradable, moreover, in high concentration, and it is demanding to select the standard method to reduce the dye waste before throwing it into the environment. Therefore, pre-treatment before being sent away is fundamental. Traditional methods, such as precipitation, were applied to overcome this trouble. Other inventive techniques to treat this waste have also been developed, bearing research using photocatalytic

degradation [5-7], chemical oxidation [8-9] activated carbon [10], metal-organic framework (MOF) [10-11], and adsorption [12-13].

Based on the current information, adsorption is one of the covenant procedures that is commercially efficient, flexible, and practical for removing textile dyes from wastewater [14]. This method is low-cost and straightforward and does not need toxic organic solvents [15]. Another benefit of this non-destructive method is low energy consumption; it uses no pre-treatment method and environmentally friendly materials that can be applied [16]. One introductory study of the adsorption method is the adsorbent's performance, so selecting the adsorbent type is essential. One of the crucial parameters for the adsorption method is the adsorbent's characteristic. The advantage of bio-sorbents is that they are cheap and they apply green chemistry principal. Bio-sorbents from crops, i.e., almond skin and olive waste, have been applied as nanoparticle-activated carbon. It can absorb some pollutants, but having a nanomaterial structure is sometimes complex and costly. Hence, looking for a low-cost and safe alternative adsorbent with good capacity adsorption for the environment is crucial. In an earlier study, almond shells [4] and banana peels [17] were used as bio-sorbent for RhB. The research revealed that the shells of almond trees and the adsorption capacity of banana skins were insufficient.

The most popular beverage worldwide is tea, "*Camellia sinensis*." Daily consumption of tea reaches twenty billion cups [18]. Catechins and flavanol are the compounds in the tea that can be anti-oxidants. The mineral content in tea includes magnesium, potassium, flour, sodium, calcium, zinc, manganese, and copper. Furthermore, the classification of tea includes black, oolong, green, white, pure, and dark tea. The withering and oxidation processes can produce different varieties of tea. Many reports of tea commodity show that it has numerous health benefits such as anticancer, cholesterol reduction, antibacterial properties, anti-inflammatory, and contribution agent to weight loss [19]. Due to its potential, extensive research has concluded that tea waste is an appropriate bio-sorbent for reducing dyes and heavy metals in wastewater.

Cellulose, lignin, tannin, and structural proteins are the chemical compounds found in tea [20]. Specific functional groups effectively form physicochemical reactions with heavy metals and some pollutants. This property helps as a tool to remove hazardous contaminants from wastewater. Green tea (GT) flavonoids are higher than Black tea (BT). So, the adsorption capacity could be higher. The –OH functional group of cellulose in tea may form a hydrogen bond with the carbonyl group of RhB.

Therefore, this work uses batch adsorption experiments to examine the efficiency of BT and GT in RhB adsorption. Specific parameters to be analyzed are adsorption study, isotherm, thermodynamics, and adsorption kinetics. BT and GT morphologies were studied using SEM analysis. The primary objective of this research is to enhance the economic value of tea waste by reducing the toxic dye concentration in wastewater.

■ EXPERIMENTAL SECTION

Materials

Most of the devices used in this study were easy to access in most laboratories. The materials used are Rhodamine-B (RhB) (99% purity Merck, CAS 81889), sodium hydroxide (NaOH) (99% purity Sigma Aldrich, 415413), hydrochloric acid (HCl) (Merck, CAS 7647-01-0), acetic acid glacial (Merck, CAS 64-19-7), aquadest, black tea, and green tea used in this study were purchased from a market in Indonesia.

Procedure

BT and GT characterization

Besides the primary instruments, an Agilent 8453 UV-Vis Spectrophotometer, Fourier Transform Infra-Red Spectrophotometer (IR Prestige-21 Fourier Transform Infrared Spectrophotometer Shimadzu) and Scanning Electron Microscope (SEM SU3500) were also utilized for the purpose. Initially, both tea wastes were cleaned and boiled in water for 8 h and put in the oven at 105 °C to dry overnight. Then, both dry tea wastes were grounded until getting a particle size of 80 mesh. The batch method was used to study the interaction of

RhB with GT and BT bio-sorbent. This study focuses on contact times, temperatures, pH, and concentrations. The BT and GT adsorption characteristics were studied at pH 1.0 to 7.0, 10–60 min of contact time, 30–100 °C of temperature, and 0.5 to 4 mg/L for RhB as the initial dye concentrations.

The methods are described as follows: 0.2 g of BT and GT waste are added to several Erlenmeyer. After that, 10 mL of RhB dye B 5 mg L^{-1} is added. The mixture is stirred for 10 to 60 min. After that, the mixture was centrifuged for 60 min at 4000 rpm. The absorbance of the filtrate was measured at its maximum wavelength of 543 nm [17]. The calculation of the concentration of the absorbed dye is prepared. The result indicates an uptake curve as a function of contact time. Subsequently, the optimal contact time for the absorption of the dye was achieved. The temperature change was measured in the same manner as the contact time. Furthermore, the immersion conditions were performed during the optimal contact period. The pH effect has been investigated under optimal contact time and temperature conditions. During this time, the effect of the initial dye concentration is evaluated at the optimum contact time, temperature, and pH.

RhB solutions with different initial concentrations in particular volumes were transferred to Erlenmeyer and then stirred in a mechanical shaker at 4000 rpm with a mass of bio-sorbent for an optimum contact time. The standard spectrophotometric method was used to calculate the RhB concentration. The batch method data was obtained to calculate the equilibrium RhB adsorptive quantity using the following expression (Eq. (1)):

$$qt = \frac{V}{m}(C_0 - C_t) \quad (1)$$

where q_t is the RhB adsorbed per g of bio-sorbent (mg/g) at time t, V is the volume treated, C_t is the RhB concentration in solution (mg/L) at time t, C_0 is the initial RhB concentration in solution (mg/L), and m is the mass of bio-sorbent weight. Furthermore, a scanning electron microscope (SEM) was used to study the morphology of GT and BT.

Study of adsorption isotherm

Equilibrium adsorption isotherms were achieved by stirring 10 mg of BT and GT with 5 mg L^{-1} of RhB solutions of different initial concentrations (5–50 mg L^{-1}). The dye concentration in the solution and adsorption capacity was calculated as described above.

Kinetics of adsorption

The kinetic study was done by stirring 10 mg of BT and GT with 10 mL of 5 mg L^{-1} RhB solutions, individually, at the same constant speed and optimum pH (the pH of the solution was selected as the optimum from the pH experiment). Samples were detached at appropriate time intervals (10, 20, 30, 40, and 50 min), and the absorbance in the supernatant was measured. The concentration of the dye in the solution and its adsorption capacity was determined as described above.

Study of thermodynamic

Batch experiments were treated with 10 mg L^{-1} RhB solutions and mixed with 10 mg of BT and GT at different temperatures (323 K until 327 K) to study the thermodynamics of the adsorption.

■ RESULTS AND DISCUSSION

Adsorption Mechanism

Bio-sorbents BT and GT, which contain polysaccharide or polyphenol, have -OH functional groups, which may form ester bonds with the carbonyl group (C=O) of RhB (Fig. 1). Such a reaction mechanism will lead to concluding that the adsorption mechanism was chemisorption. Such a reaction mechanism was supported by studying the liquid phase adsorption of RhB onto Chitosan [21]. In addition to chemisorption, the reaction of cellulose with RhB is also possible for physisorption. It can be assumed that the N atom from the RhB group will interact to form hydrogen bonds with the -OH group of cellulose.

Characterization of the BT and GT

SEM analysis

SEM studies the physical properties, morphology, and analysis method of organic and inorganic materials

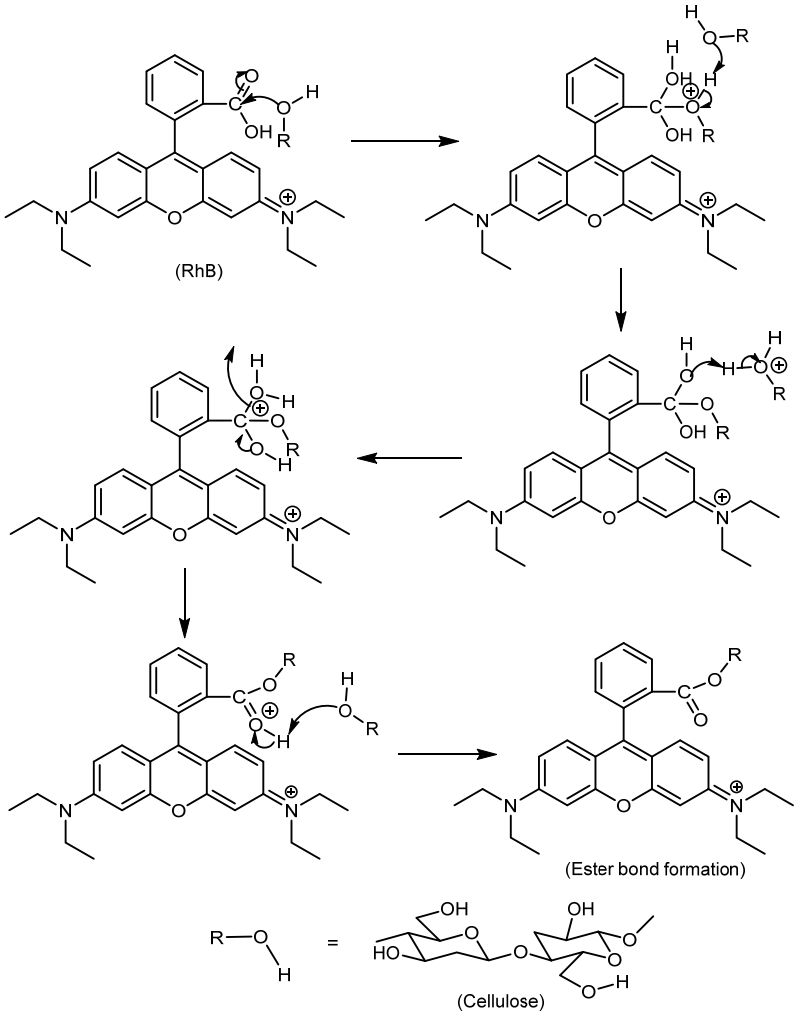

Fig 1. Possible reaction mechanism between cellulose from bio-sorbent and RhB

on a nanometer scale to micrometer (μm) of the GT and BT [22]. The SEM micrograph of BT and GT before and after adsorption with RhB was acquired at a resolution of 20.000× magnification using a particle size of 1 μm. The surface morphology of BT and GT after adsorption with RhB (Fig. 2(b) and (d)) conformed narrowly different than before adsorption with RhB (Fig. 2(a) and (c)).

In Fig. 2(a) and (c), the micrograph displayed a mesh structure of the GT and BT morphology. After adsorption (Fig. 2(b) and (d)), the SEM morphology of GT and BT showed new network structures when RhB is diffused into the pores. The particles were compactly packed with no apparent open porous surface, which proved that chemical modification of the surface or interaction between bio-sorbent and the RhB dye had taken place. The results were similar to other reports [17,23].

FTIR analysis

One of the essential topics that must be investigated is the mechanism of RhB adsorption on GT and BT as active functional groups on the surface of the adsorbent are involved in chemical reactions during the adsorption process. To address this problem, FTIR analysis is therefore required. Fig. 3 shows the usual FTIR spectra before and after RhB reacts with the BT and GT samples. According to Fig. 3(a), the characteristic peak of O–H and N–H was seen in BT at 3400 cm^{-1}, which is associated with polyphenol stretching modes [24]. Alcohol derivatives and phenolic substances contain hydroxy functional groups, as shown

by wavenumbers that broaden in the 3300 cm^{-1} areas. Areas in phenolic compounds and alcohol derivatives show the presence of hydroxy functional groups. The functional group of the carbonyl (C=O) bond stretching and the double bond of carbon (C=C) in an aromatic circle were linked to the strong peak at 1600 cm^{-1}. Stretching of alkane (C–H and O–H) was found at wavelength 2900 cm^{-1}, while carboxylic acid was given adsorption in an area of 2800 cm^{-1}. Apart from that, the C–O stretching in amine emerged at 1000 cm^{-1}. Identical results were found from a previous study [25], where the results of the FTIR analysis of tea samples also found absorption at 3388, 1636, and 1039 cm^{-1}, indicating the presence of a hydroxide group, primary amine, double bond C, and also

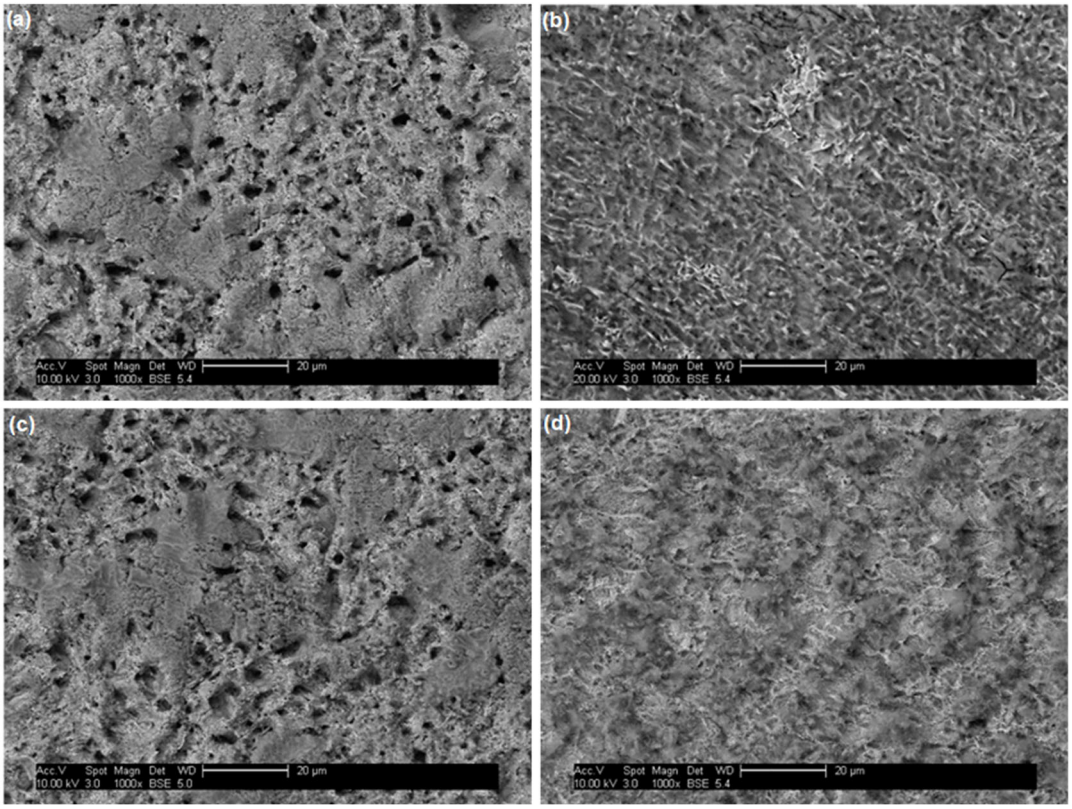

Fig 2. SEM Image of black tea (a), black tea-RhB (b), green tea (c), green tea-RhB (d)

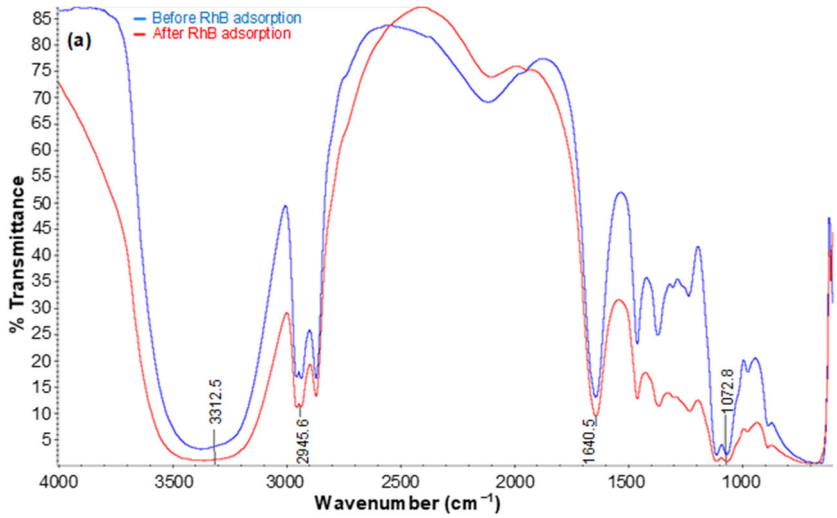

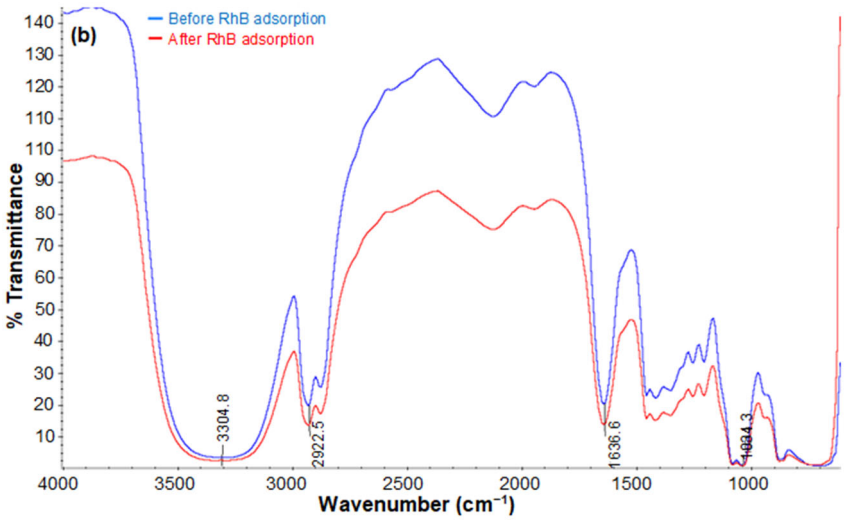

Fig 3. FTIR Spectra of black tea (a) and green tea (b)

the presence of an ether group (C–O–C), respectively. This shows that polyphenol, carboxylic acid, and amino acid compounds are the main functional groups present in tea samples.

The IR range of GT (Fig. 3(b)) was compared to BT; the band at 3300 cm^{-1} appeared, extending vibrations of O–H bunches in water, liquor, and phenols, and N–H extending in amines. The C–H extension in alkanes and the O–H extension in carboxylic corrosive show up at 2900 and 2800 cm^{-1}, respectively. The solid band at 1600 cm^{-1} was credited to the C=C extension within the aromatic ring and the C=O extension in polyphenols. The C–N extend of amide gives the band at 1300 cm^{-1}. The C–O–C extending in polysaccharides gives a band at 1700 cm^{-1}, and C–O extending in amino acids causes a band at 1000 cm^{-1}. Polyphenols, carboxylic corrosive, and polysaccharides are plenteous in BT and GT. Fig. 3(a) and 3(b) appear the FTIR range of BT and GT sometime recently and after RhB adsorption. The carbonyl extends of C=O of ester from RhB shows up at 1650 cm^{-1}. The new C=O bond shape emphatically impacted the retention of RhB. The shape of the groups (Fig. 3(a) and (b)) remains unaltered but for an increment within the absorbance after cellulose responds with RhB. This portrayal takes after a past ponder [26]. Absorbance gets to be higher and % transmittance after adsorption of RhB into BT and GT diminishes. It affirms that these utilitarian bunches tie the RhB color through chemical interactions.

Effect of Contact Time

Fig. 4 shows how contact time affects adsorption capacity. As much as 0.2 g of each BT and GT were mixed with 5 mg L^{-1} RhB solution (pH 2). The contact time interval is 10 to 60 min. Adsorption increases significantly in the first ten minutes. Adsorption is fast initially and slows down near equilibrium. This finding is supported by previous studies, which found that color removal was rapid in the early stages of contact time and decreased over time [4]. As can be seen from Fig. 4(a), 40 min is the equilibrium time before adsorption remains constant. In 40 min, the adsorption capacity of BT and GT was 0.8 and 1.22 mg/g, respectively. Iryani et al. [15] found that the adsorption process stays higher during a contact time of about 80 min. While adsorption of RhB using nanoparticle-modified surfactants achieves a faster contact time of about 30 min [27].

Effect of Temperature

Five mg L^{-1} RhB (pH 2) was stirred for 40 min with the BT and GT at different temperatures (30–100 °C). Fig. 4(b) shows that the adsorption capacity is small at 0.2 mg/g (BT) and 0.38 mg/g (GT) at 30 °C. As the temperature increases, it affects the adsorption capacity and reaches the optimal adsorption at 80 °C, while for BT at 70 °C. The capacity showed 1.2 and 0.8 mg/g for GT and BT, respectively. Theoretically, at high temperatures, the adsorbent surface leads to more contact

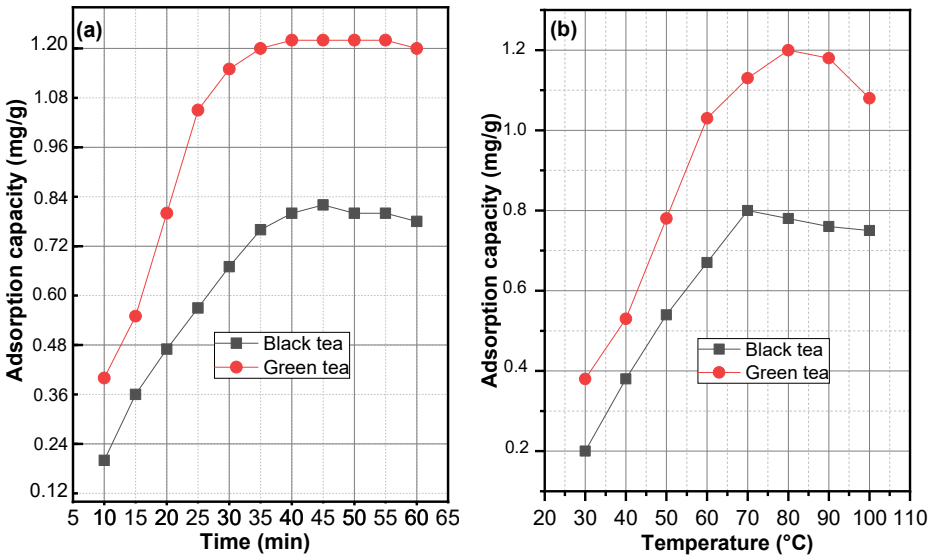

Fig 4. Effect of contact time on the adsorption of RhB on the BT and GT 5 mg L^{-1}, pH 2, adsorbent dose 0.2 g, temperature 25 °C (a) and effect of temperature on the adsorption of RhB on BT and GT 5 mg L^{-1}, pH 2.0; contact time 40 min, adsorbent dose 0.2 g, temperature 25 °C (b)

with the adsorbate. This phenomenon can be explained by the movement of RhB molecules at high temperatures. These data were found to be similar to previous research [28]. RhB adsorption decreased due to increased Brownian motion. It can be explained that the hydrogen bond between RhB and bio-sorbent has a significant potential to break. This finding was found similar to previously reported work [15,21]. An increase in temperature may have led to a reduction in the binding force between the adsorbent and RhB, thereby reducing the adsorption capacity of the adsorbent at high temperatures.

Effect of pH

The effect of pH (1–7) was performed to support this study. As one of the crucial parameters, pH affects the adsorption performance of RhB on BT and GT, as it involves the reaction between the anion and the cation on the surface of the adsorbent. Based on previous studies, adsorption of RhB on orange peel powder, the optimal pH was reached at pH 3. In our study, optimization was limited from pH 1 to 7 [29]. The optimal sorption of RhB at pH values between 3 and 4 has been addressed previously [21].

A 0.2 g BT and GT were examined with 5 mg L^{-1} RhB dye solutions for 40 min. In Fig. 5(a), it can be observed that the adsorption percentage increases as the pH of the RhB solution increase from 1 to 2 folds by multiples. The pH reached the optimum at 2.5 for BT and GT with a degree of adsorption of 85.0 and 93.6%, respectively. These findings were also supported by the previous study [30]. The effect of H^+ ions does not affect absorption at low pH. Therefore, the capacity of cellulose adsorption remains high. The presence of OH^- under alkaline conditions inhibits the absorption of RhB. This can be explained by the OH competition between the surface of the adsorbent and OH– from the solution. The -OH group reacts with the carbonyl group (C=O) of RhB. These phenomena cause the adsorption capacity to become low [30]. This phenomenon has also been reported [21].

When the pH of the RhB solution is low, the bio-sorbent is rich in positive ions, and then the adsorption capacity becomes low. The repulsion between the cationic RhB molecules and the positively charged absorbent surface. As the pH of the RhB solution slowly increases, the number of hydroxyl ions increases. Therefore, the adsorption capacity increases. This can be explained by the form of attraction between cationic RhB and cellulose in the bio-sorbent. While RhB exists in its zwitterionic form above pH 3.7, it forms larger molecules (dimers)

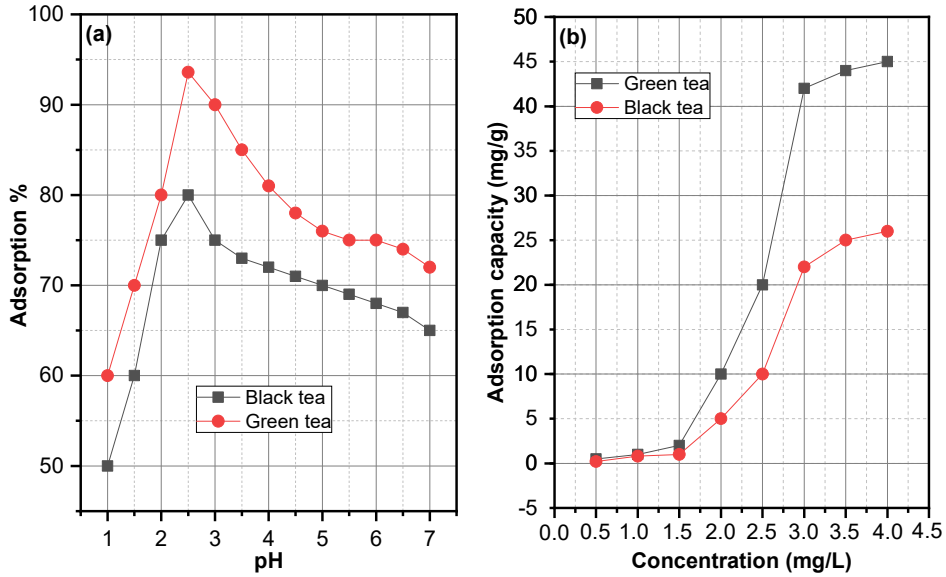

Fig 5. Effect of pH on the adsorption of RhB on BT and GT 5 mg L^{-1}, contact time 40 min, adsorbent dose 0.2 g, temperature 25 °C (a) and effect of initial concentrations of RhB on the adsorption of BT and GT pH 2.5, contact time 40 min, adsorbent dose 0.2 g; temperature 25 °C (b)

between the carboxyl and xanthene groups of RhB; thus, the adsorption capacity becomes low.

Effect of Initial Dye Concentration

The RhB (0.5 to 4 mg L^{-1}) was used to study the effect of increasing concentration on the adsorption capacity. Fig. 5(b) describes the graph between the initial concentration and the adsorption capacity in mg/g. It explained that as the initial concentrations of the dyes increased, the amount of RhB adsorbed also increased. The trend of the curve reaches constant when the concentration of both bio-sorbents is 3 mg L^{-1}. As RhB concentration increases, so does the driving force of gradient concentrations [28]. Our results showed that increasing RhB concentration increases the adsorption capacity from 0.2 to 22 mg/g and 0.5 to 47 mg/g for BT and GT, respectively. Rather and Sundarapandian and Sebeia et al. [31-32] reported that the adsorption sites are saturated because there are limited binding sites applicable on the adsorbent surface.

Adsorption Isotherm

Adsorption isotherms describe the amount of adsorbate retained on an adsorbent surface at a fixed temperature when the system reaches equilibrium. Adsorption isotherms are fundamental to optimizing and understanding the use of an adsorbent. Additionally, studying isotherms can help to elucidate the adsorption mechanism between the adsorbent (BT and GT) and the adsorbate (RhB). Equilibrium data were analyzed using Freundlich and Langmuir isotherm models. According to Langmuir, adsorption takes place at homogeneous points of the adsorbent, and Freundlich achieves a heterogeneous surface of the adsorbent with non-uniform distribution of the heat of adsorption over the surface [29]. Eq. (2) defines the logarithmic form of the Freundlich model, and Eq. (3) shows the Langmuir equation [33].

$$\log Q_e = 1/n \log C_e + \log K_F \quad (2)$$

where Q_e is the amount of adsorbate at equilibrium (mg/g), C_e is the equilibrium concentration of the adsorbate (RhB), K_F is the Freundlich constant related to adsorption capacity, and n is the constant related to the intensity of adsorption proportionated with the heterogeneity factor. The plots of log Q_e vs. log C_e ought to present a linear graph, and the value of n and K_F can gain from the slope and intercept of the graph, respectively.

$$\frac{C_e}{Q_e} = \frac{C_e}{q_{max}} + \frac{1}{K_L \cdot q_{max}} \quad (3)$$

The q_{max} represents an equilibrium RhB concentration (mg/g) while K_L relatives to the adsorption capacity (mg/g) is the Langmuir constant. K_L is matched with the appropriate range variation and adsorbent porosity. The adsorption capacity becomes high because of the large surface area and pore volume. The RhB isothermal adsorption model on BT and GT was statistically evaluated by the R^2 shown in Fig. 6(a) and (b). The linear regression of BT and GT was 0.9967 and 0.9979, respectively (Fig. 6(b)). By comparing its R^2, the Langmuir better described the adsorption of RhB. It proves that the adsorption of RhB was monolayer adsorption. The Langmuir isotherms give maximum adsorption capacities of 12.5 and 20.0 mg/g for BT and GT, respectively.

The factor of separation (the dimensionless equilibrium parameter), R_L, is used to confirm the favorability of the adsorption that occurs. When the R_L value is between 0 and 1, that is to say ($0 < R_L < 1$) and $R_L = 1$ mean that the adsorption process is favorable. While $R_L = 0$ means the adsorption process is irreversible, and when $R_L > 1$ means the adsorption is unfavorable [29]. The R_L can be examined as Eq. (4) [33]:

$$R_L = \frac{1}{1 + bC_0} \quad (4)$$

where b shows the constants of Langmuir and C_0 is the initial dye concentration (mg mL^{-1}). The R_L values based on calculations were 0.026 and 0.055, respectively, which means that the adsorption process was favorable.

Adsorption of RhB using a hybrid ion exchanger follows the Langmuir model; The capacity of the Langmuir isotherm was 76.4 mg/g at 25 °C [34]. Another study used banana peel to remove RhB, and the result shows that the maximum adsorption capacity (Q_{max}) was 9.522 mg/g, which was suitable for the Langmuir model [17]. Adsorption of RhB followed the Langmuir isotherm model in graphene oxide. The adsorption capacity was 8.69 mol g^{-1}, and the R_L was found in the range of 0–0.01 [35]. As well as the research with orange peel powder for the adsorption of RhB follows the Langmuir model [29].

Adsorption Kinetics

The pseudo-first order (Eq. (5)) and the pseudo-second order (Eq. (6)) models were used to study the kinetic study of BT and GT:

$$\log(q_e - q_t) = \log q_e - \frac{k_1}{2.303}t \quad (5)$$

$$\frac{t}{q_e} = \frac{1}{k_2 q_e^2} + \frac{t}{q_e} \quad (6)$$

where q_t and q_e are the amount of solute sorbed per mass of bio-sorbent (mg/g) at any time and equilibrium, respectively, and k_1 is the rate constant of first-order sorption (min^{-1}). The plot of log ($q_e - q_t$) vs. t gives slope

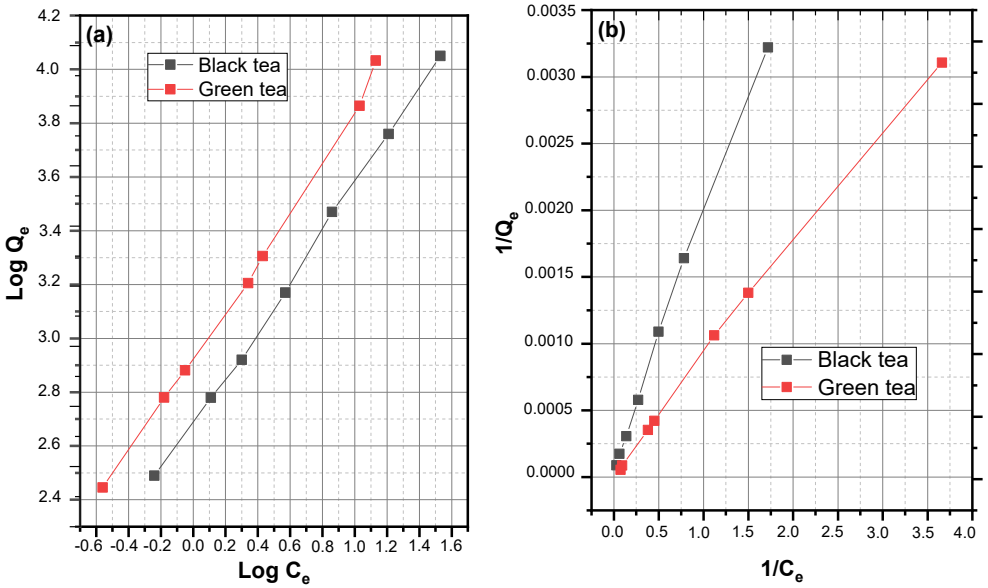

Fig 6. Freundlich (log C_e vs log Q_e) (a) and Langmuir ($1/C_e$ vs $1/Q_e$) (b) isotherm graphs

for log (q_e) and intercepted as the plot of log ($q_e - q_t$). In comparison, k_2 (g mg^{-1} min^{-1}) shows the rate constant of the pseudo-second order model [36].

Pseudo-first order and pseudo-second order models of RhB adsorption have been described in Fig. 7(a) and (b). Table 1 shows BT and GTs kinetic parameters after RhB adsorption. The intercepts and slopes that can indicate all kinetic parameters are presented in Table 1. BT and GT have a linear regression of 0.9869 and 0.9929, respectively, for a pseudo-first order kinetic model. The pseudo-second order model (Fig. 7(b)) shows 0.9989 and 0.9963 for BT and GT, respectively. From this, it can be concluded that the regression linearity of the pseudo-second order kinetics is higher than the pseudo-first order kinetics. Therefore, this study follows the pseudo-second order kinetic model. The capacity adsorption of *Moringa oleifera* seeds to Cu(II) and Pb(II) follows the pseudo-second order model [36]. A similar result occurs with the adsorption of *Casuarina equisetifolia* cone powder to RhB [37].

Adsorption Thermodynamics

The thermodynamics were studied for the adsorption of RhB onto BT and GT, including parameters such as standard Gibbs energy change (ΔG°), enthalpy change (ΔH°), and entropy change (ΔS°). These parameters express the spontaneity, feasibility, and interaction between the sorbate-sorbent. The relationship between ΔG°, ΔH° and ΔS° was calculated using Eq. (7).

$$\left[\frac{d\ln C_e}{d(1/T)}\right]_\theta = \frac{\Delta H_{ads}}{R} \quad (7)$$

where θ demonstrates the fraction of surface coverage and ΔH° is the enthalpy of adsorption. For a specific amount adsorbed, the effect of equilibrium concentrations with temperature has been described in Fig. 6(a). The adsorption enthalpy was calculated from the

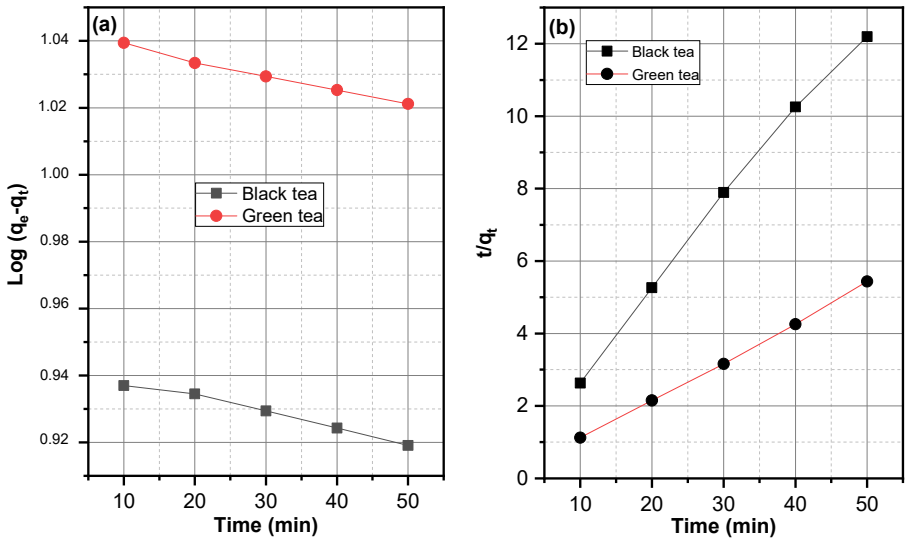

Fig 7. Pseudo-first order (a) and pseudo-second order (b) kinetics of BT and GT

Table 1. Parameters of adsorption isotherms and kinetic model

	Adsorption isotherm		Kinetic model	
	Freundlich	Langmuir	Pseudo-first order	Pseudo-second order
Black tea	R^2 = 0.9988	R^2 = 0.9967	R^2 = 0.9869	R^2 = 0.9989
	K_F = 480.40 (μg/g)(L/mg)$^{1/n}$	Q_{max} = 12.50 mg/g	Q_e = 8.76 mg/g	Q_e = 158.73 mg/g
	1/n = 0.8915	b = 2.6 × 10^{-2} L/mg	K_1 =1.15 × 10^{-3} min^{-1}	K_2 = 3.7 × 10^{-4} g mg^{-1} min^{-1}
Green tea	R^2 = 0.9965	R^2 = 0.9979	R^2 = 0.9929	R^2 = 0.9963
	K_F = 928.32 (μg/g)(L/mg)$^{1/n}$	Q_{max} = 20.00 mg/g	Q_e =11.04 mg/g	Q_e = 238.09
	1/n = 0.8252	b = 5.5 × 10^{-2} L/mg	K_1 = 9.2 × 10^{-4} min^{-1}	K^2 = 4.28 × 10^{-5} g mg^{-1} min^{-1}

plot of ln C_e vs. 1/T, as shown in Fig. 8. It was studied at some temperatures. The straight line shows the slope of the plot, which corresponds to the ΔH°/R, while ΔS°/R is equal to the intercept. Whereas R (8.314 kJ mol^{-1} K^{-1}) is the gas constant and T is the absolute temperature, respectively. The ΔG°, ΔH°, ΔS° values obtained are described in Table 2.

The value of ΔH° at pH 2.5 based on calculation, was -63.33 and -64.13 kJ mol^{-1}, respectively, indicating that the adsorption of Rh-B on BT and GT followed an exothermic process (at higher temperatures, the adsorption reaction is less favorable). The calculated value of ΔH° was more than 40 kJ mol^{-1}, indicating that the adsorption mechanism was chemisorption, as predicted in Fig. 1. ΔH° for physisorption is between 20 and 40 kJ mol^{-1} [38].

ΔS° with a positive value indicates that RhB adsorption on BT and GT increases. This occurs due to increased disorder at the interface between the analyte and the bio-sorbent. With increasing temperatures, the degree of disorder in the adsorbate-adsorbent interactions compared to the adsorbate-solvent interaction increases. Eq. (8) was used to obtain the ΔG° value of adsorption.

$$\Delta G^\circ = \Delta H^\circ - T\Delta S^\circ \quad (8)$$

Based on the calculation, the ΔG° values reached -6.917 and -5.959 kJ mol^{-1} for BT and GT, respectively. A negative ΔG° indicates improved feasibility and spontaneity of the RhB bio-sorbent system at elevated temperatures [39]. This result agrees with a report by Bankole et al. [40]. A study comparison of tea waste as a bio-sorbent in this work compared to other adsorbents (Table 3) describes that GT has a higher adsorption capacity.

Removal Study

The removal study was used to get information about the regeneration of BT and GT and reusability after the adsorption experiment and find out the adsorption mechanism on RhB. The eluents used in the removal study were water, acetic acid, and sodium hydroxide 1 M. The efficiency of each eluent was measured by calculating the RhB concentration desorbed from BT and GT to the RhB concentration in RhB-loaded bio-sorbents using Eq. (9) [40].

$$\text{Efficiency of desorption} = \frac{Q_{de}}{Q_{ad}} \times 100 \quad (9)$$

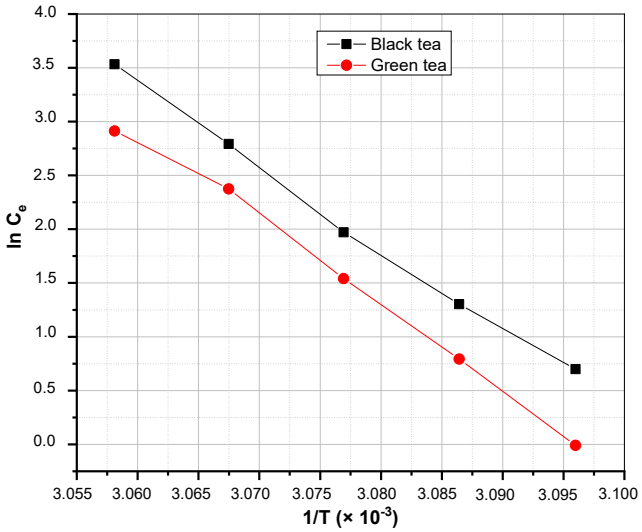

Fig 8. A Plot of ln C_e vs 1/T × 10^{-3} for adsorption of RhB into BT and GT

Table 2. Thermodynamic parameters

	T (K)	ΔG° (kJ/mol)	ΔH° (J/mol)	ΔS° (J/mol K)
Black tea	298	-6.917	-63.33	23.00
Green tea	298	-5.959	-64.13	199.7

Table 3. Comparison of RhB adsorption on different various low-cost and green adsorbent

Adsorbent	Adsorption capacity (mg/g)	References
Coffee ground powder	5.26	[2]
Paper waste	6.71	[42]
Banana peel	9.52	[17]
Black tea	22.0	This study
Green tea	47.0	This study

Q_{de} is the concentration of RhB desorbed by eluents, and Q_{ad} is the concentration of RhB adsorbed into bio-sorbent. Estimated desorption efficiencies for BT for water, sodium hydroxide, and acetic acid (10%) were 10.01, 47.89, and 59.06%, respectively. While for GT the desorption efficiencies were 12.96, 50.45, and 60.23%, respectively, which can be concluded that solvents that can regenerate the bio-sorbent increase the desorption efficiency. Therefore, acetic acid (10%) has better adsorption properties than sodium hydroxide and water. Another study reported that 75% of the methylene blue could be desorbed from the surface of Fe_3O_4 bound to graphene oxide using 5% acetic acid in a methanol solution [41].

■ CONCLUSION

The adsorption process taking place on the surface of the adsorbent is chemisorption using a single-layer mechanism, while the reaction process taking place kinetically follows the pseudo-second order type. The presence of an exothermic reaction is indicated by the negative value of the thermodynamic parameter (ΔG°). A negative value for the change in ΔS° suggests that the degree of disorder decreases as the adsorption process occurs; thus, energy must be expended since this does not happen spontaneously. Based on the findings, the cheaply available and environmentally friendly waste products, i.e., tea waste products, will be a good alternative for industries using such dye removal in the future.

■ ACKNOWLEDGMENTS

The author thanks the State Islamic University (UIN) Syarif Hidayatullah Jakarta and the Ministry of Energy and Mineral Resources for the support gained for this research.

■ AUTHOR CONTRIBUTIONS

All authors contributed evenly to this project. Meyliana Wulandari and Nofrizal performed the experiment and calculations, writing and revising the manuscript. Syed Azhar Syed Sulaiman is proofreading this manuscript.

■ REFERENCES

[1] Postai, D.L., Demarchi, C.A., Zanatta, F., Melo, D.C.C., and Rodrigues, C.A., 2016, Adsorption of rhodamine B and methylene blue dyes using waste of seeds of *Aleurites moluccana*, a low cost adsorbent, *Alexandria Eng. J.*, 55 (2), 1713–1723.

[2] Shen, K., and Gondal, M.A., 2017, Removal of hazardous Rhodamine dye from water by adsorption onto exhausted coffee ground, *J. Saudi Chem. Soc.*, 21 (Suppl. 1), S120–S127.

[3] Saigl, Z.M., 2021, Various adsorbents for removal of rhodamine B dye: A review, *Indones. J. Chem.*, 21 (4), 1039–1056.

[4] Abdolrahimi, N., and Tadjarodi, A., 2019, Adsorption of rhodamine-B from aqueous solution by activated carbon from almond shell, *Proceedings*, 41 (1), 51.

[5] Varadavenkatesan, T., Lyubchik, E., Pai, S., Pugazhendhi, A., Vinayagam, R., and Selvaraj, R., 2019, Photocatalytic degradation of rhodamine B by zinc oxide nanoparticles synthesized using the leaf extract of *Cyanometra ramiflora*, *J. Photochem. Photobiol., B*, 199, 111621.

[6] Xu, D., and Ma, H., 2021, Degradation of rhodamine B in water by ultrasound-assisted TiO_2 photocatalysis, *J. Cleaner Prod.*, 313, 127758.

[7] Zheng, S., Ding, B., Qian, X., Yang, Y., Mao, L., Zheng, S., and Zhang, J., 2022, High efficiency degradation of tetracycline and rhodamine B using Z-type $BaTiO_3$/γ-Bi_2O_3 heterojunction, *Sep. Purif. Technol.*, 278, 119666.

[8] El Khames Saad, M., Rabaaoui, N., Elaloui, E., and Moussaoui, Y., 2016, Mineralization of *p*-methylphenol in aqueous medium by anodic oxidation with a boron-doped diamond electrode, *Sep. Purif. Technol.*, 171, 157–163.

[9] Khadhri, N., Ben Mosbah, M., Rabaaoui, N., Khadimallah, M.A., and Moussaoui, Y., 2021, Advancements of electrochemical removal of *o*-methylphenol from aqueous using BDD anode compared to Pt one: Kinetics and mechanism

determination, *Iran. J. Chem. Chem. Eng.*, 40 (5), 1446–1456.

[10] Khadhri, N., El Khames Saad, M., Ben Mosbah, M., and Moussaoui, Y., 2019, Batch and continuous column adsorption of indigo carmine onto activated carbon derived from date palm petiole, *J. Environ. Chem. Eng.*, 7 (1), 102775.

[11] Paiman, S.H., Rahman, M.A., Uchikoshi, T., Abdullah, N., Othman, M.H.D., Jaafar, J., Abas, K.H., and Ismail, A.F., 2020, Functionalization effect of Fe-type MOF for methylene blue adsorption, *J. Saudi Chem. Soc.*, 24 (11), 896–905.

[12] Alghamdi, A.A., Al-Odayni, A.B., Saeed, W.S., Almutairi, M.S., Alharthi, F.A., Aouak, T., and Al-Kahtani, A., 2019, Adsorption of azo dye methyl orange from aqueous solutions using alkali-activated polypyrrole-based graphene oxide, *Molecules*, 24 (20), 3685.

[13] da Silva Filho, S.H., Vinaches, P., and Pergher, S.B.C., 2018, Zeolite synthesis in basic media using expanded perlite and its application in rhodamine B adsorption, *Mater. Lett.*, 227, 258–260.

[14] Brião, G.V., Jahn, S.L., Foletto, E.L., and Dotto, G.L., 2017, Adsorption of crystal violet dye onto a mesoporous ZSM-5 zeolite synthetized using chitin as template, *J. Colloid Interface Sci.*, 508, 313–322.

[15] Iryani, A., Nur, H., Santoso, M., and Hartanto, D., 2020, Adsorption study of rhodamine B and methylene blue dyes with ZSM-5 directly synthesized from Bangka kaolin without organic template, *Indones. J. Chem.*, 20 (1), 130–140.

[16] El-Azazy, M., El-Shafie, A.S., and Yousef, B.A.S., 2021, Green tea waste as an efficient adsorbent for methylene blue: Structuring of a novel adsorbent using full factorial design, *Molecules*, 26 (20), 6138.

[17] Oyekanmi, A.A., Ahmad, A., Hossain, K., and Rafatullah, M., 2019, Adsorption of Rhodamine B dye from aqueous solution onto acid treated banana peel: Response surface methodology, kinetics and isotherm studies, *PLoS One*, 14 (5), e0216878.

[18] Hussain, S., Anjali, K.P., Hassan, S.T., and Dwivedi, P.B., 2018, Waste tea as a novel adsorbent: A review, *Appl. Water Sci.*, 8 (6), 165.

[19] Jeyaseelan, C., and Gupta, A., 2016, Green tea leaves as a natural adsorbent for the removal of Cr(VI) from aqueous solutions, *Air, Soil Water Res.*, 9, ASWR.S35227.

[20] Bansal, M., Patnala, P.K., and Dugmore, T., 2020, Adsorption of Eriochrome Black-T (EBT) using tea waste as a low cost adsorbent by batch studies: A green approach for dye effluent treatments, *Curr. Res. Green Sustainable Chem.*, 3, 100036.

[21] Inyinbor, A.A., Adekola, F.A., and Olatunji, G.A., 2017, Liquid phase adsorptions of rhodamine B dye onto raw and chitosan supported mesoporous adsorbents: Isotherms and kinetics studies, *Appl. Water Sci.*, 7 (5), 2297–2307.

[22] Garcia-Betancourt, M., Magaña-Zavala, C., and Crespo-Sosa, A., 2018, Structural and optical properties correlated with the morphology of gold nanoparticles embedded in synthetic sapphire: A microscopy study, *J. Microsc. Ultrastruct.*, 6 (2), 72–82.

[23] Yi, W.S., Qin, L.H., and Cao, J.B., 2011, Investigation of morphological change of green tea polysaccharides by SEM and AFM, *Scanning*, 33 (6), 450–454.

[24] Brza, M.A., Aziz, S.B., Anuar, H., Ali, F., Dannoun, E.M.A., Mohammed, S.J., Abdulwahid, R.T., and Al-Zangana, S., 2020, Tea from the drinking to the synthesis of metal complexes and fabrication of PVA based polymer composites with controlled optical band gap, *Sci. Rep.*, 10 (1), 18108.

[25] Huang, L., Weng, X., Chen, Z., Megharaj, M., and Naidu, R., 2014, Synthesis of iron-based nanoparticles using oolong tea extract for the degradation of malachite green, *Spectrochim. Acta, Part A*, 117, 801–804.

[26] Navarro, J.R.G., and Bergström, L., 2014, Labelling of *N*-hydroxysuccinimide-modified rhodamine B on cellulose nanofibrils by the amidation reaction, *RSC Adv.*, 4 (105), 60757–60761.

[27] Yen Doan, T.H., Minh Chu, T.P., Dinh, T.D., Nguyen, T.H., Tu Vo, T.C., Nguyen, N.M., Nguyen, B.H., Nguyen, T.A., and Pham, T.D., 2020, Adsorptive removal of rhodamine B using novel

adsorbent-based surfactant-modified alpha alumina nanoparticles, *J. Anal. Methods Chem.*, 2020, 6676320.

[28] Dinçer, A., Sevildik, M., and Aydemir, T., 2019, Optimization, isotherm and kinetics studies of azo dye adsorption on eggshell membrane, *Int. J. Chem. Technol.*, 3 (1), 52–60.

[29] Daouda, A., Honorine, A.T., Bertrand, N.G., Richard, D., and Domga, D., 2019, Adsorption of rhodamine B onto orange peel powder, *Am. J. Chem.*, 9 (5), 142–149.

[30] Hossain, M.A., and Alam, M.S., 2012, Adsorption kinetics of Rhodamine-B on used black tea leaves, *Iran. J. Environ. Health Sci. Eng.*, 9 (1), 2.

[31] Rather, M.Y., and Sundarapandian, S., 2022, Facile green synthesis of copper oxide nanoparticles and their rhodamine-B dye adsorption property, *J. Cluster Sci.*, 33 (3), 925–933.

[32] Sebeia, N., Jabli, M., Ghith, A., and Saleh, T.A., 2020, Eco-friendly synthesis of *Cynomorium coccineum* extract for controlled production of copper nanoparticles for sorption of methylene blue dye, *Arabian J. Chem.*, 13 (2), 4263–4274.

[33] Ayawei, N., Ebelegi, A.N., and Wankasi, D., 2017, Modelling and interpretation of adsorption isotherms, *J. Chem.*, 2017, 3039817.

[34] Saruchi, S., and Kumar, V., 2019, Adsorption kinetics and isotherms for the removal of rhodamine B dye and Pb^{+2} ions from aqueous solutions by a hybrid ion-exchanger, *Arabian J. Chem.*, 12 (3), 316–329.

[35] Sahar, J., Naeem, A., Farooq, M., Zareen, S., and UrRahman, A., 2019, Thermodynamic studies of adsorption of rhodamine B and Congo red on graphene oxide, *Desalin. Water Treat.*, 164, 228–239.

[36] April, M., Kowanga, K.D., Gatebe, E., Mauti, G.O., and Mauti, E.M., 2016, Kinetic, sorption isotherms, pseudo-first-order model and pseudo-second-order model studies of Cu(II) and Pb(II) using defatted *Moringa oleifera* seed powder, *J. Phytopharm.*, 5 (2), 71–78.

[37] Kooh, M.R.R., Dahri, M.K., and Lim, L.B.L., 2016, The removal of rhodamine B dye from aqueous solution using *Casuarina equisetifolia* needles as adsorbent, *Cogent Environ. Sci.*, 2 (1), 1140553.

[38] Malana, M.A., Ijaz, S., and Ashiq, M.N., 2010, Removal of various dyes from aqueous media onto polymeric gels by adsorption process: Their kinetics and thermodynamics, *Desalination*, 263 (1-3), 249–257.

[39] Nawi, M.A., Sabar, S., Jawad, A.H., Sheilatina, S., and Wan Ngah, W.S., 2010, Adsorption of reactive red 4 by immobilized chitosan on glass plates: Towards the design of immobilized TiO_2-chitosan synergistic photocatalyst-adsorption bilayer system, *Biochem. Eng. J.*, 49 (3), 317–325.

[40] Bankole, O.M., Oyeneyin, O.E., Olaseni, S.E., Akeremale, O.K., and Adanigbo, P., 2019, Kinetics and thermodynamic studies for rhodamine B dye removal onto graphene oxide nanosheets in simulated wastewater, *Am. J. Appl. Chem.*, 7 (1), 10–24.

[41] Zhou, C., Zhang, W., Wang, H., Li, H., Zhou, J., Wang, S., Liu, J., Luo, J., Zou, B., and Zhou, J., 2014, Preparation of Fe_3O_4-embedded graphene oxide for removal of methylene blue, *Arabian J. Sci. Eng.*, 39 (9), 6679–6685.

[42] Thakur, A., and Kaur, H., 2017, Response surface optimization of rhodamine B dye removal using paper industry waste as adsorbent, *Int. J. Ind. Chem.*, 8 (2), 175–186.